sciendo

**Journal of Smart Internet of Things (JSIoT)**
**VOL 2023, No.02 | 62-83 | 2023**
**DOI: 10.2478/jsiot-2023-0011**

*Article*

# Modelling of African Vulture Optimization Algorithm with Deep Learning-based Object Classification for Intelligent Manufacturing Systems

Ameer N. Onaizah[1], Mohanad R. Aljanabi[2]

[1] Beijing Institute Of Technology, School Of Automation, zhongguancun ,Beijing,100811, China
[2] Kharazmi University, College of Mathematical Sciences and Computer, Tehran, Iran

*Corresponding author: Ameer N. Onaizah (email: ameer@bit.edu.cn)

Received 05 September 2023; Accepted 22 October 2023; Issue Published 15 December 2023

**Abstract:** Intelligent manufacturing system incorporates a number of sensors including IoT devices, cameras, and scanners, for capturing real-time data about the manufacturing process. Based on their physical properties, colours, dimensions, or other relevant characteristics, these sensors can be used to track and identify waste objects. Waste object classification in intelligent manufacturing includes the usage of recent systems and technologies to detect and classify waste materials or objects produced during the manufacturing process. The objective is to enable effective waste management and recycling practices, optimizing resource utilization and reducing environmental impact. Manual waste classification is a laborious and expensive task, which results in the development of automatic waste classification models using artificial intelligence (AI) techniques. It remains a challenging process due to the significant variations in the solid waste because of varying shapes, colours, and sizes. Therefore, recent advances in deep learning (DL) methods can be employed to accomplish the solid waste classification process. The study introduces a chaotic African vulture optimization algorithm with a deep learning-based solid waste classification (CAVOA-DLSWC) system. The CAVOA-DLSWC technique aims to automatically detect waste objects and classify them into different categories using DL models. In the presented CAVOA-DLSWC approach, two major processes are involved such as object classification and detection. For the object detection method, the CAVOA-DLSWC technique uses a lightweight RetinaNet model with CAVOA based hyperparameter tuning process. The CAVOA is derived by integrating the chaotic concepts into the initial iteration values of the AVOA. Once the waste objects are identified, the classification process can be performed by the use of convolutional long short-term memory (CLSTM) network. The experimental values of the CAVOA-DLSWC approach can be tested employing the solid waste database including diverse kinds of waste objects. The comparative results show the remarkable performance of the CAVOA-DLSWC method over other techniques.

**Keywords:** Intelligent manufacturing; Solid waste management; Deep learning; Computer vision; Waste recycling; Plastic waste

Copyright © 2023 Journal of Smart Internet of Things (JSIoT) published by Future Science for Digital Publishing and Sciendo . This is an open access article license CC BY (https://creativecommons.org/licenses/by/4.0/)

## 1. Introduction

Intelligent manufacturing system leverages data analytics and pattern recognition techniques to analyze a wide range of sensor data. By relating different patterns and variables, it becomes possible to detect specific patterns or waste objects related to waste production [1]. Then, these data can be used to minimize waste production and enhance manufacturing processes. An intelligent manufacturing system integrates the capabilities of waste object classification with the overall manufacturing infrastructure. This integration allows real-time monitoring and feedback loops, enabling immediate action to be taken once the waste object was detected [2]. It triggers an automated process for sorting, reusing, or recycling waste materials, thus reducing waste disposal costs and optimizing resource utilization. This system provides manufacturers with insight and recommendations on waste reduction strategies, process optimization, and sustainable practices. The manufacturers can make informed decisions to improve overall operational efficiency and minimize waste by leveraging the classified waste object data [3]. Plastic waste is the main concern because of long-term environmental degradation. Prompt measures are required to enable wise collection and segregation of garbage, to prevent environmental pollution, and consequently, to protect the life of wild organisms and humans [4].

Actions targeted at minimalizing the quantity of waste generated and placed in the environments must include the procedure of modern low-waste or non-waste technologies, recycling raw materials [5], changing conventionally used raw materials, and minimalizing waste production. Nonwaste technology (NWT) prevents waste and complete use of raw materials. It includes more technological procedures that result in complete management, followed by the removal of pollution without detrimental effects on the surroundings [6]. The NWT implementation has its economic justification since the reduction of the amount of waste and complete use of materials paves the way for better productivity and reduces the imports of raw materials [7]. Rarely, it may probably minimalize the usage of heat and electricity or by decreasing energy-consuming waste treatment procedures. The benefits of utilizing non-waste technology include reducing operating costs, material consumption, and environmental losses. Machine learning (ML) emerges as one potential means to support waste sorting [8]. Nowadays, ML-related systems that could support sorting methods have been applied, hastening this procedure. The frequently utilized solution is smart self-sorting waste bins that categorize single objects placed on a background at a time [9]. If one compartment is utilized, the camera is situated at the topmost place in the upper container. The deep learning (DL) method allocates the right class depending on the image, and the trash is relocated to the correct bottom container [10].

The study introduces a chaotic African vulture optimization technique with a deep learning-based solid waste classification (CAVOA-DLSWC) technique. The CAVOA-DLSWC technique aims to automatically detect waste objects and classify them into different categories using DL models. In the presented CAVOA-DLSWC approach, two major processes are involved, such as object classification and detection. For the object detection method, the CAVOA-DLSWC technique uses lightweight RetinaNet model with CAVOA based hyperparameter tuning process. The CAVOA is derived by integrating the chaotic concepts into the initial iteration values of the AVOA. Once the waste objects are identified, the classification process can be performed by the use of convolutional long short-term memory (CLSTM) network. The experimental values of the CAVOA-DLSWC system can be tested employing the solid waste database comprising diverse types of waste objects.

## 2. Related Works

The authors [11] develop a novel DL-related small object identification and categorization technique for handling garbage waste method (DLSODC-GWM). The suggested procedure majorly concentrates on identifying and categorizing minimal garbage waste particles in helping intellectual waste handling structures. The presented method follows two main procedures called Object Detection (OD) and categorization. Wang et al. [12] employ the DL-based categorizer and cloud computing (CC) method to achieve huge precision waste categorization at the beginning of Garbage Collection (GC). To ease the corresponding disposal of the garbage, the author segments biodegradable garbage into six classes, namely paper, glass, fabric, cardboard, metal, plastic, and other re-processable garbage. DL convolution neural networks (DLCNN) were practiced in realizing the waste categorizing duty. In [13], an elaborated characterization was made of the prevailing DL methods that have been suggested to categorize garbage. This research suggests a style for the categorization of clutter into the classifications defined in the standard methods. The style employed for the categorization was EfficientNet-B0. This paper suggests the EfficientNet-B0 method of tuning for images precise to certain demographic areas for effective categorization.

In the article [14], a CNN-based method named YOLO is implemented as the OD protocol to ease the categorization of garbage accordant to several classifications at the point of garbage grouping. In addition, a Nature Inspired (NI) pursuit procedure is implemented as a learning frequency for the CNN method. The implementation of NI search models, like the Kestrel-based Search Algorithm (KSA), has demonstrated imminent anticipation related to learning frequency parameter determination in garbage OD and categorization. Khan et al. [15] have employed an ultrasonic sensor, Arduino UNO microcontroller, and moisture sensor. Anyone could measure the garbage index of a specific discarding ground by employing image processing. A hardware model was established for the suggested context. The article [16] intends in establishing an automatic garbage categorization method by trying conventional and DL machine methods. To accomplish that, both created a database and open Trashnet are employed in testing and exercising. JONET DL method has been established by adopting a grouping of the pre-educated base method (DenseNet201) with a new style that consists of a complete interrelated level in the categorization phage with 1024 neurons. The method is proficient in recognizing six modules of dense garbage substances with several precisions.

The article [17] implements ML protocols and the existing research-established methods for anticipating the products of non-catalytically procedures and constant procedures for the pyrolysis of garbage plastics. In addition, Gaussian Process (GP), Support Vector Machine (SVM), Decision Tree (DT), and Artificial Neural Network (ANN) have four different approaches with a diverse input database, used to select input parameters for the greatest precise methods. Amongst these methods, the DT method displayed acceptable and generalizable exactness ($R2 > 0.99$) with a training record.

## 3. The Proposed Model

In this manuscript, a novel CAVOA-DLSWC model has been introduced for a robust waste classification model, which helps to improve recycling productivity. The CAVOA-DLSWC technique follows a three-stage process: Lightweight RetinaNet object detector, CAVOA-based hyperparameter tuning, and CLSTM-based object classification. Fig. 1 displays the working flow of the CAVOA-DLSWC methodology. The complete working of these modules is elaborated below:

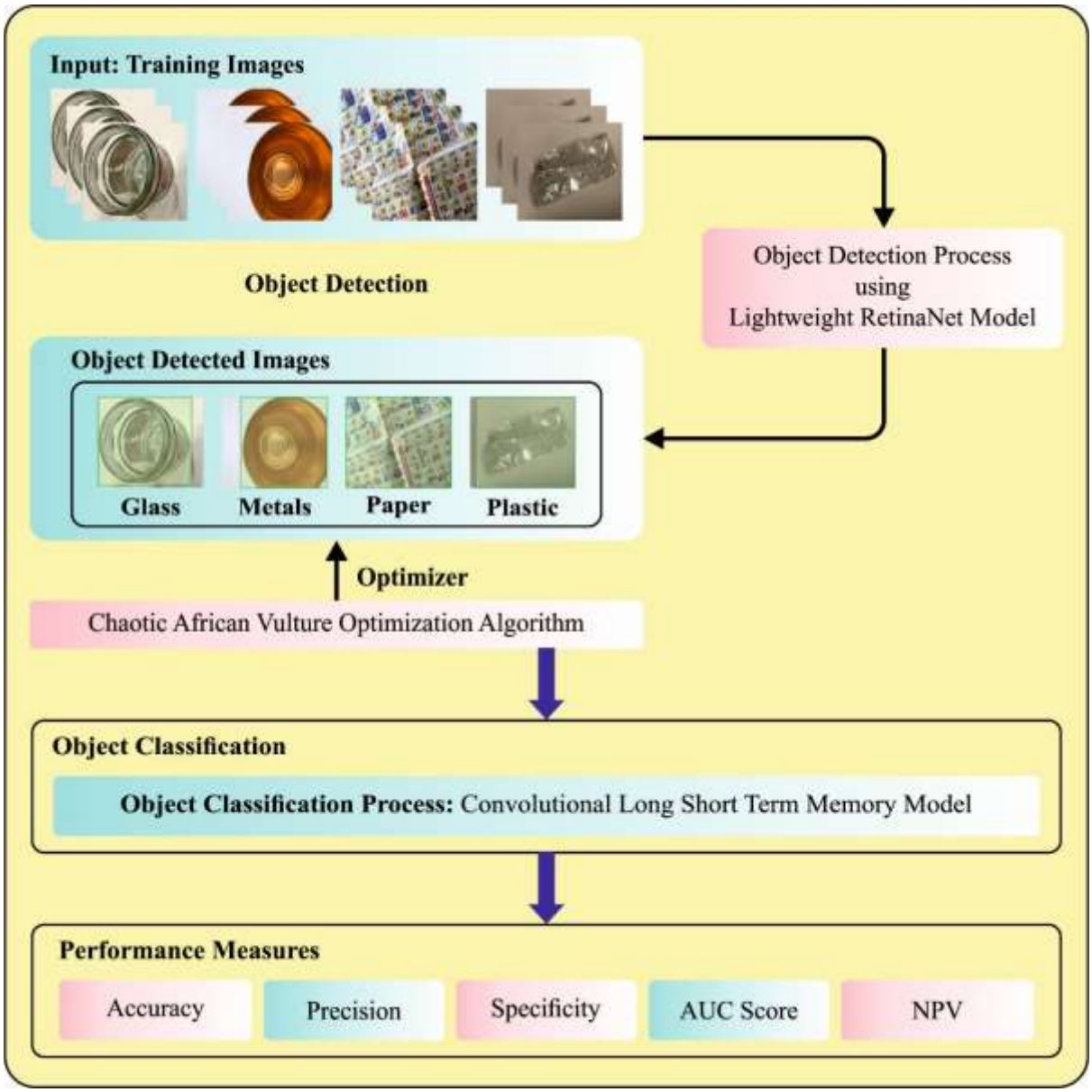



Figure 1: Workflow of CAVOA-DLSWC approach

### *3.1 Stage I: Object Detection Module*

In this work, the lightweight RetinaNet model effectually detects waste objects. RetinaNet module includes a backbone, Feature Pyramid Network (FPN), and a detection backend [18]. At first, the image was handled by means of a backbone that is usually a ResNet module. It should be noted that MobileNet efficacy is on par outstanding with ResNet with regard to the classification; it isn't sufficiently accurate to be perceived as an equivalent replacement for ResNets. Fig. 2 shows the structure of RetinaNet. From this point of view, MobileNet is exploited as a backbone for the detection process, although it undergoes lower accuracy in classification outcomes. The main objective is that the confidence score of MobileNet-based backbone is minimized by trade-off with the lowest computational cost. Consequently, the desirable option isn't considered as the backbone of an extremely precise object detection model. The subsequent FPN and The backbone are combined to form encoding and decoding networks. FPN has the benefits, viz., it integrates the

features of the succeeding layer in the hardest to the finest level such that the feature in distinct levels and scales are powerfully transferred to the succeeding layer. Then, the several scale pyramid features ($P3 - P7$) are fed to the backend, where both detection subsections are exploited for bounding box regression and object classification.

The filter size is minimized for accomplishing the reduction of FLOP. At this point, the D-blockv1 exploits the MobileNet model. A 3x3 depthwise convolutional layer and a 1x1 convolution layer exchange one new layer. The D-block-v2 successively places 1x1 in addition to 3x3 kernels. According to YOLOv1, replace the 3x3 kernels without giving the residual block. In the presented method, the filter counts is set to the constant value over the layers. The D-block-v3 has been extremely aggressive since it replaces all the 3x3 convolutions with the 1x1 convolutional layer. In these scenarios, the lightweight block undergoes a reduction in performance for trading off lesser computation costs. In the RetinaNet architecture, the fully-shared weight model can be replaced by the partially-shared weight model to compensate for the accuracy reduction. A partially shared weight model mainly consists of two advantages. Additionally, D3 has an independent weighted accuracy parameter that learns personalized features for the branch and could compensate for the reduction by lower computational complexity.

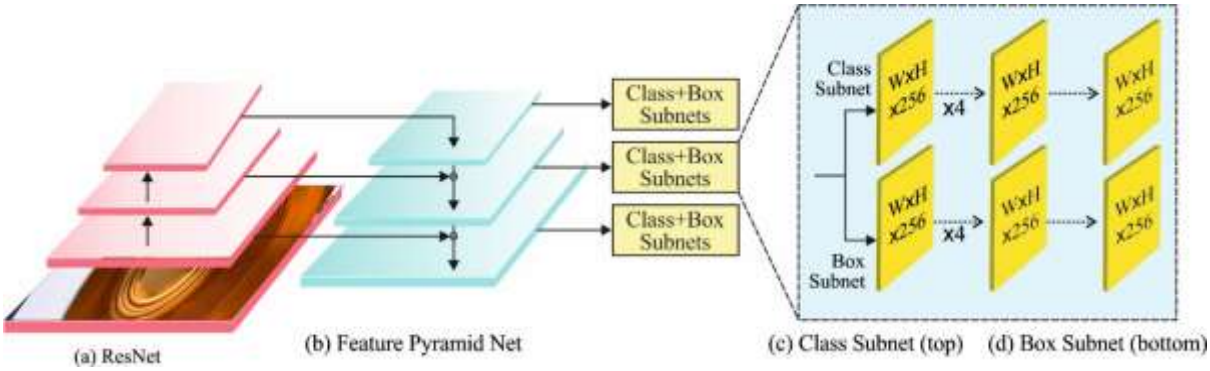



Figure 2: Structure of RetinaNet

### *3.2 Stage II: Parameter Tuning Module*

The CAVOA technique is used to adjust the hyperparameter value of the lightweight RetinaNet architecture. AVOA is stimulated through the natural behaviors of the rare species of African vultures [19]. The population includes $N$ vultures demonstrating promising solutions to optimization problems. The population is divided into two major groups. The AVOA includes 4 different phases. The initial stage begins with the initial randomization of all individuals from population between the upper along with the lower boundaries of every optimization parameter. But random initialization causes few individuals to be distant from the optimum solution; thus, the model does not reach the optimal solution or even converges slower. The chaotic optimization technique was utilized for population initialization. The chaotic logistic mapping technique defines the population initialization. This perturbation helps to explore region of the search space. Presenting chaos in the process of searching makes the algorithm more likely to identify the global minima and less likely to be stuck in local minima. The chaotic logistic mapping can be mathematically expressed below:

$$y(1) = rand, \tag{1}$$
$$y(i+1) = ry(i)(1 - y(i)).$$

In Eq. (1), $r$ denotes the characteristic variable of logistic map, whose value has been fixed as 4, and $rand$ shows the random integer within [0,1]. Then, the population can be initialized by the succeeding formula, which considered upper bound ($UB$) and the lower bound ($LB$) of the optimizer variable:

$$P(i) = y(i).(UB - LB) + LB. \quad (2)$$

In Eq. (2), $P$ indicates the location of all the vultures, and counter $i$ from 1 to $N$. Also, the initial stage involves the vultures' separation into two groups. Afterwards, population initialization and the fitness of each vulture should be evaluated. Next, the optimal vulture (minimum fitness value) was selected to be the better one of initial group ($Best_Vulture_1$), whereas the second best vulture from entire population can be chosen as $Best_Vulture_2$ (second group's best vulture ). It becomes crucial to arbitrarily select the better vulture from both groups that are further utilized in the exploration and exploitation stages. These random vultures are characterized as $(i)$, and it is selected based on the succeeding formula:

$$R(i) = \begin{cases} Besf_Vulture_1, p_i = L_1 \\ Besf_Vulture_2, p_i = L_2 \end{cases} \quad (3)$$

In Eq. (3), $p_i$ represents the likelihood of selecting the better vulture from the initial or the second groups, and it can be attained by Roulette wheels. To retain a balance between global and local search processes, the variables $L_1$ and $L_2$ were selected so that its sum equals 1. Then, the starvation of the vulture should be inspected. For these purposes, the satiation rate $F$ can be evaluated by Eq. (32):

$$F = t + z(1 + 2r_1)\left(1 - \frac{ite}{max_{ite}}\right), \quad (4)$$

$$t = h(\sin^w(\frac{\pi}{2}(\frac{ite}{max_ite})) + \cos(\frac{\pi}{2}(\frac{ite}{max_ite})) - 1).$$

Where $z$ signifies a random integer in the [-1, 1], $ite$ and max_$it$ indicated the current iteration and maximal amount of iterations, correspondingly, $r_1$ signifies a random integer in zero and one, and $h$ signifies an arbitrary value in [- 2, 2]. The satiation rate $F$ was critical since it determines the subsequent stage. If $|F| \geq 1$, then the vulture searches for food in different regions of the search region in the exploration stage. If $|F| < 1$, the vulture only finds food in the nearby region of the existing solution that relates to the exploitation stage. Next, the exploration stage depends on two different approaches. The $P_1$ parameter is used to select the suitable approach. Right before exploration takes place, a random integer $rcmd_{P1}$ is within [0,1]; if that random value is lesser than the predetermined variable $P_1$, the initial exploration stage is utilized. Or else the model employs a second exploration phase. Thus, the vulture position can be upgraded by Eq. (5):

$$P(ite + 1) = \begin{cases} R(ite) - |XR(ite) - P(ite)|F, P_1 \geq rand_{P1} \\ R(ite) - F + rand_2\big((UB - LB)rand_3 + LB\big), P_1 < rand_{P1} \end{cases} \quad (5)$$

Vector coefficient $X$ is introduced to improve the random motion. It is evaluated by $X = 2rand$, where $rand$ is a vector of random integers within [0,1]. As well, $rcmd_2$ and $rcmd_3$ denote random numbers ranging from zero to one. From the abovementioned, when $|F| < 1$, the exploitation stage takes place, where the technique concentrates on local search. Two exploitation stages are potential based on $|F|$. In addition, all the stages include two approaches. The AVOA approach enters the initial exploitation stage if $|F|$ is between 0.5 and 1. In such cases, the pre-determined value $P_2$, which should be between 0 and 1, is used for choosing the strategy. Random integer $rcmd_{P2}$ declares the applied strategy to update the position of the vulture:

$$P(ite + 1) = \begin{cases} |X.R(ite) - P(ite)|(F + rand_4) - (R(ite) - P(ite)), P_2 \geq rand_{P2} \\ R(ite) - (S_1 + S_2), P_2 < rand_{P2} \end{cases} \quad (6)$$

Where the terms $S_1$ and $S_2$ are determined by Eq. (35):

$$S_1 = R(ite)\left(\frac{rand_5 P(ire)}{2\pi}\right)\cos(P(ire)), \quad (7)$$

$$S_2 = R(ite)\left(\frac{rand_6 P(ire)}{2\pi}\right)\sin\left(P(ire)\right).$$

Like the previous equation, $rand_5$ and $rand_6$ represent random number ranges from [0,1]. When $|F| is < O.5$, this method entered the second exploitation stage. This stage begins with creating arbitrary integer $rand_{P3}$ within [0,1] and compared to the variable $P_3$ that is already established. Thus, the position of the vulture is upgraded based on the subsequent conditions:

$$P(ite+1) = \begin{cases} \frac{A_1 + A_2}{2}, P_3 \geq rand_{P3} \\ R(ite) - |R(ite) - P(ite)|F - y(R(ite) - P(ite)), P_3 < rand_{P3} \end{cases} \quad (8)$$

The *terms* $A_1$ and $A_2$ characterize the gathering of the vulture from 2 groups over the food source, as follows:

$$A_1 = Best_Vulture_1(ite) - \frac{Best_Vulture_1(ite)P(ite)}{Best_Vulture_1(ite) - P(ite)^2}F, \quad (9)$$

$$A_2 = Best_Vulture_2(ite) - \frac{Best_Vulrure_2(ite)P(ite)}{Best_Vulture_2(ite) - P(ite)^2}F.$$

AVOA employs the Levy flight patterns like other metaheuristic approaches to improve its effectiveness:

$$Levy\ (x) = 0.01\left(\frac{u.\sigma}{|\iota fm|^{1/\beta}}\right), \sigma = \left(\frac{\Gamma(1+\beta)\sin\left(\frac{\pi\beta}{2}\right)}{\Gamma\left(\frac{1+\beta}{2}\right)2^{\frac{\beta 1}{2}}\beta}\right)^{1/\beta} \quad (10)$$

In Eq. (10), $u\ and\ \iota$ denotes random number ranging from zero to one, and $\beta$ is a fixed variable equivalent to 1.5.

Lastly, the *overall* process for a single iteration was complete. The process reiterates till the maximal amount of iterations can be attained. Furthermore, the optimum solution of the optimization problem is characterized by the parameter $Best_Vulture_1$. For optimal parameter selection process, the CAVOA technique determines a fitness value according to the fitness function (FF), defined in Eq. (11). The fitness value implies a positive integer, which directly indicates the effectual outcomes of the candidate solutions. In the presented CAVOA-DLSWC technique, the FF aims to reduce the classifier error rate.

$$fitness(x_i) = ClassifierErrorRate(x_i) = \frac{No.of\ misclassified\ instances}{Total\ no.of\ instances} * 100 \quad (11)$$

**Algorithm 1:** Pseudocode of the CAVOA algorithm

Input datasets: the maximal amount of iterations and population size
Initialized the population by chaotic logistic mapping using Eqs. (1) and (2)
*while* $(ite <$ max$_ite)$
Compute the fitness of the entire population and decide $Best_Vulture_1$ and $Best_Vulture_2$
For all vultures from the population
Define $R$ utilizing (3)
Upgrade $F$ utilizing (4)
if $|F| \geq 1$ then exploration phase
Upgrade the locations utilizing (5)
Otherwise, enter the exploitation stage

If $|F| \geq 0.5$, enter the initial exploitation stage
Upgrade the locations utilizing (6)
Otherwise, enter the second exploitation stage
Upgrade the locations utilizing (8)
End if
End if
End for
End while

### *3.3 Stage III: Object Classification Module*

The CLSTM model is utilized in this work for the waste classification process. The CLSTM element integrates the CNN and LSTM networks [20]. The CNN comprises 2 convolutional (Conv) layers, and the LSTM network involves 2 LSTM layers, correspondingly. An input of CLSTM is input data matrix $X_t^S$ that signifies the historical input data of POI that forecast and its neighbours. The 1D-Conv function is applied to data flow $X_t^S$ at every time step $t$ to extract the spatial feature. A 1D Conv kernel filtering can be exploited for acquiring the local perceptual domain by sliding filtering. The development of Conv kernel filtering was formulated as:

$$Y_t^S = \sigma(W_s * X_t^S + b_s), \tag{12}$$

In which $W_s$ stands for the filtering weights, $b_s$ represents the bias, $X_t^S$ denotes the input data at time $t$, the symbol $*$ defines the Conv function, $\sigma$ refers to the activation function, and $Y_t^S$ demonstrates the results of the Conv layer. The procedure was advantageous to extract the spatial feature in the neighbouring observation places.

The pooling layer could not execute the Conv layer under this method, while the dimensional spatial feature could not huge. Represent $G_t^S$ as the outcome of Conv layer 2. Afterwards, the spatial data has been modelled by 2 Conv layers, and next, the outcome was linked to the LSTM network.

An input data also demonstrates temporal connections from adjacent times. RNN is commonly established to analyze the hidden temporal features from sequential data. But, the RNN carries out worse in the event of long-term series because of the gradient vanishing problems while it forgets the previous status of sequences. An infrastructure of LSTM comprises a cell for storing block cell layer and 3 gating mechanisms such as forget input and output gates. The present state has been controlled by forgetting and input gates. LSTM utilizes the forget gate for determining that more data at the prior cell layer was reserved from the present cell layer and utilizes the input gate for deciding that more data of input requires that stored in the present cell state. During this case, it can be present for utilizing LSTM for extracting temporal features of input data.

For enhanced the efficacy of deep neural networks (DNN), the typical approach is to enhance the layer count from the method. During this effort, it is stack several LSTM layers for modelling to capture high-level features of input data. Every LSTM layer gets the hidden layer (HL) of the prior state as its input by stacking LSTM layers. For instance, LSTM layer1 procedures the series output in the CNN element $G_t^S = [G_{t-n}^S, \dots, G_{t-1}^S, G_t^S]$ from beginning to end and computes the HL for every time-step $H_{1,t}^S = [H_{1,t-n}^S, \dots, H_1^S, {}^S{}_{H1,t}]$. Afterwards, the HL sequence $H_{1,t}^S$ is input as LSTM layer2 for estimating the HL $H_{2,t}^S$ for time step $t$ as the outcome of the whole LSTM model $H_t^S$. The calculation of every LSTM layer is defined by Eq. (13) to Eq. (17) as:

$$i_t = \sigma\left(W_{gi} I_t^S + W_{hi} H_{t-1}^S + W_{ci} \circ C_{t-1} + b_i\right), \tag{13}$$

$$f_t = \sigma\left(W_{gf} I_t^S + W_{hf} H_{t-1}^S + W_{cf} \circ C_{t-1} + b_f\right), \tag{14}$$

$$C_t = f_t \circ C_{t-1} + i_t o \tanh\left(W_{gc} I_t^S + W_{hc} H_{t-1}^S + b_c\right), \tag{15}$$

$$o_t = sigma\left(W_{go} I_t^s + W_{ho} H_{t-1}^s + W_{co} \circ C_t + b_o\right), \quad (16)$$

$$H_t^s = o_t \circ \tanh\left(C_t\right), \quad (17)$$

Whereas $C_t$ represents the cell state, $I_t^s$ implies the input of the LSTM layer at $t$ time step, $\circ$ defines the matrix element-wise product, $\sigma$ suggests the activation function, $i_t$, $f_t$, $0_t$ demonstrates the input, forget, and output at time $t$; $W$ and $b$ denote the weight and bias, correspondingly. The last resultant of LSTM layer $H_t^s$ is resolved by the output gate and upgrade cell as represented in Eq. (17). $I_t^s$ input of layer1 and layer2 are $G_t^s$ and $H_{1,t}^s$, correspondingly. The outputs $H_t^s$ of layer1 and layer2 relate to $H_{1,t}^s$ and $H_{2,t}^s$, correspondingly. Eventually, it attains the spatiotemporal feature $H_t^s$ for $t$he t time step.

## 4. Experimental Validation

In this section, we validate the waste classification performance of the CAVOA-DLSWC methodology on datasets including 4447 instances with 8 classes as exposed in Table 1. The confusion matrices of the CAVOA-DLSWC algorithm in the waste recognition process are revealed in Fig. 3. This experimental outcome shows that the CAVOA-DLSWC technique gains effectual identification of different waste objects.

**Table 1:** Details of database

| **Classes** | **No. of Images** |
|---|---|
| Background | 306 |
| Bio | 39 |
| Glass | 463 |
| Metals and Plastic | 1951 |
| Non-Recyclable | 568 |
| Other | 130 |
| Paper | 323 |
| Unknown Litter | 667 |
| **Total Samples** | **4447** |

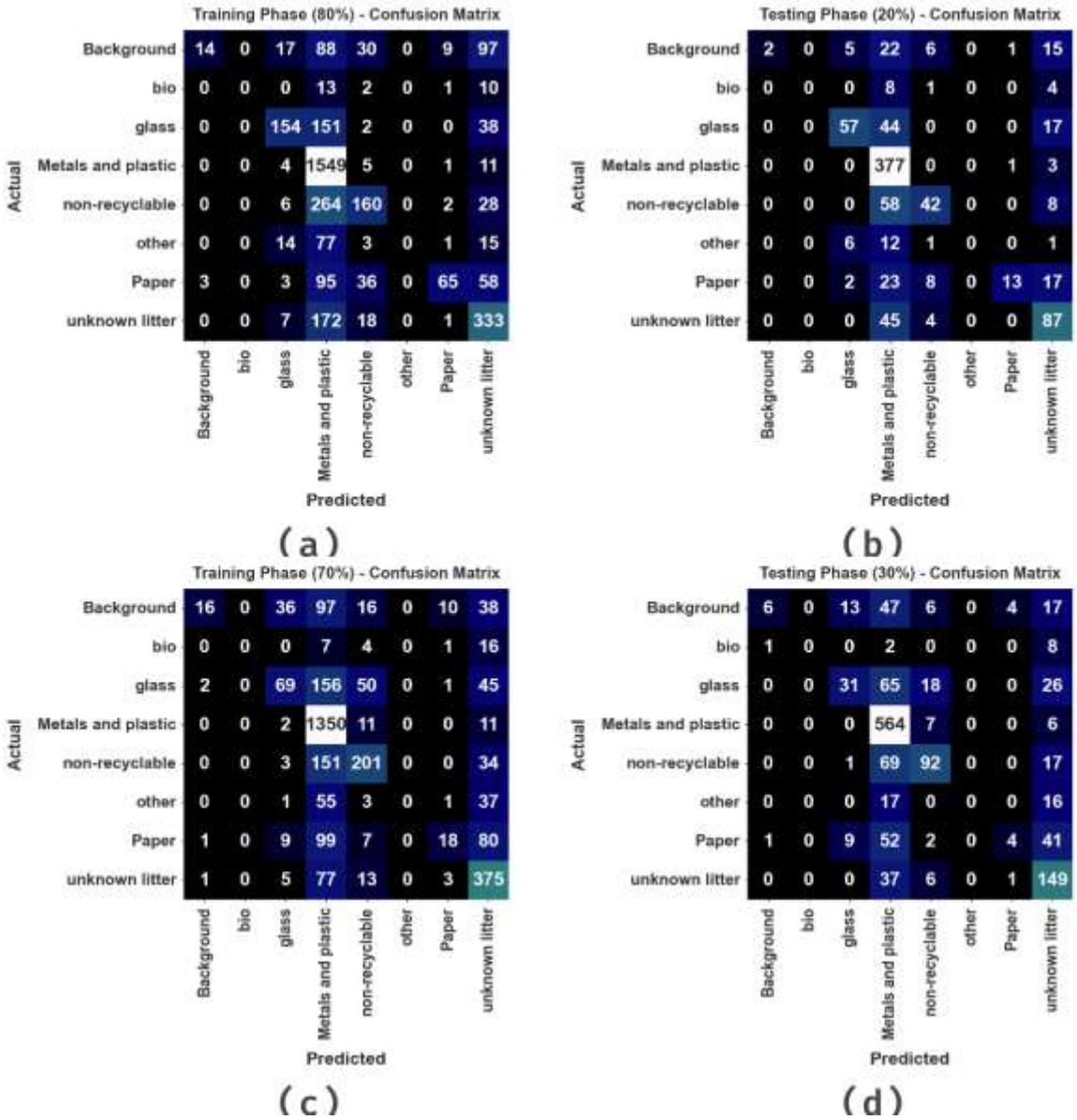



Figure 3: Confusion matrices of CAVOA-DLSWC method (a-b) TRPH/TSPH of 80:20 and (c-d) TRPH/TSPH of 70:30

The overall waste classification outcomes of the CAVOA-DLSWC model are described in Table 2 and Fig. 4. The figure illustrated that the CAVOA-DLSWC algorithm considered eight types of waste objects accurately. For instance, with 80% of TRPH, the CAVOA-DLSWC method gains an average $accu_y$ of 90.99%, $prec_n$ of 52.75%, $spec_y$ of 92.87%, $AUC_{score}$ of 63.39%, and NPV of 95.06%. Along with that, with 20% of TSPH, the CAVOA-DLSWC system gains average $accu_y$ of 91.24%, $prec_n$ of 57.14%, $spec_y$ of 93.16%, $AUC_{score}$ of 63.74%, and NPV of 95.21%.

**Table 2:** Waste classifier outcome of CAVOA-DLSWC technique with 80:20 of TRPH/TSPH

| **Class** | $Accu_y$ | $Prec_n$ | $Spec_y$ | $AUC_{score}$ | **NPV** |
|---|---|---|---|---|---|
| **Training Phase (80%)** | | | | | |
| Background | 93.14 | 82.35 | 99.91 | 52.70 | 93.19 |

| | | | | | |
|---|---|---|---|---|---|
| bio | 99.27 | 00.00 | 100.00 | 50.00 | 99.27 |
| glass | 93.20 | 75.12 | 98.41 | 71.52 | 94.30 |
| Metals and plastic | 75.23 | 64.30 | 56.72 | 77.69 | 98.17 |
| non-recyclable | 88.87 | 62.50 | 96.90 | 65.84 | 90.91 |
| other | 96.91 | 00.00 | 100.00 | 50.00 | 96.91 |
| Paper | 94.10 | 81.25 | 99.55 | 62.27 | 94.39 |
| unknown litter | 87.21 | 56.44 | 91.51 | 77.11 | 93.33 |
| **Average** | **90.99** | **52.75** | **92.87** | **63.39** | **95.06** |
| **Testing Phase (20%)** | | | | | |
| Background | 94.49 | 100.00 | 100.00 | 51.96 | 94.48 |
| bio | 98.54 | 00.00 | 100.00 | 50.00 | 98.54 |
| glass | 91.69 | 81.43 | 98.32 | 73.31 | 92.56 |
| Metals and plastic | 75.73 | 64.01 | 58.35 | 78.65 | 98.67 |
| non-recyclable | 90.34 | 67.74 | 97.44 | 68.17 | 92.03 |
| other | 97.75 | 00.00 | 100.00 | 50.00 | 97.75 |
| Paper | 94.16 | 86.67 | 99.76 | 60.20 | 94.29 |
| unknown litter | 87.19 | 57.24 | 91.38 | 77.67 | 93.36 |
| **Average** | **91.24** | **57.14** | **93.16** | **63.74** | **95.21** |

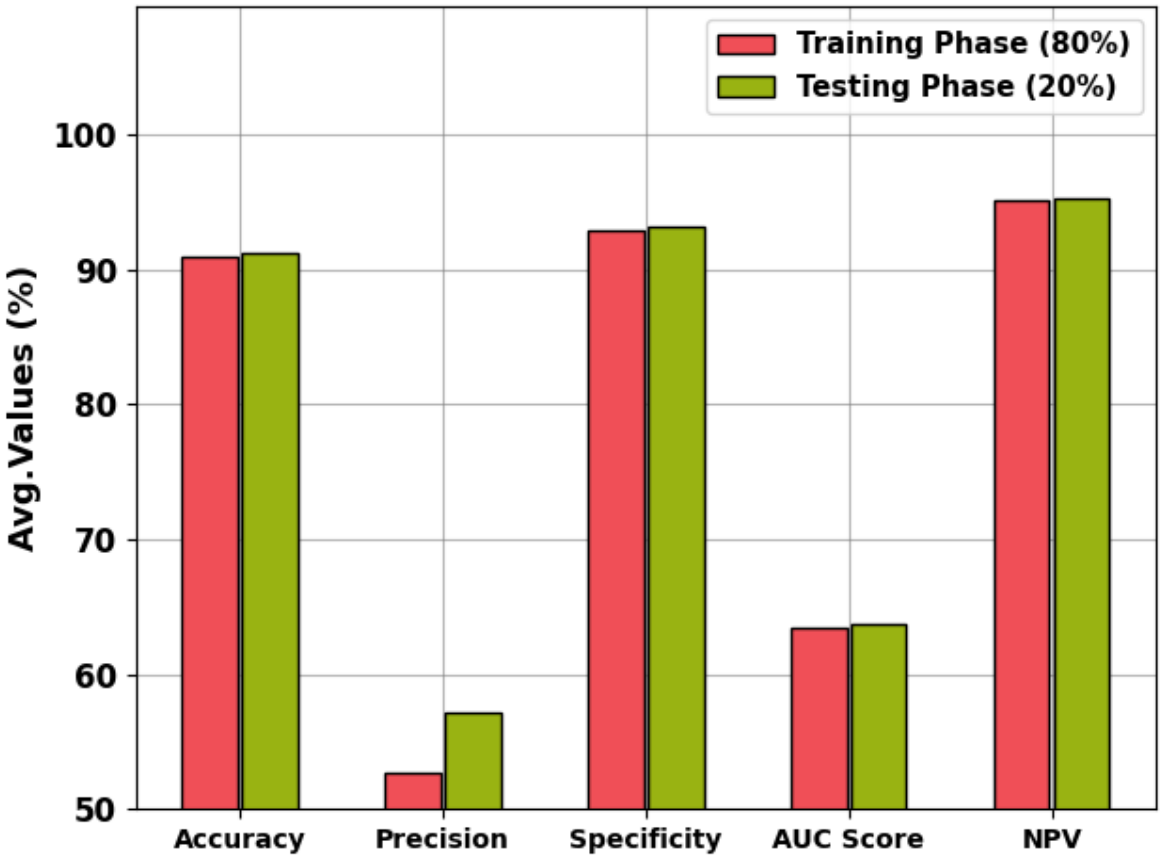



Figure 4: Average outcome of CAVOA-DLSWC approach on 80:20 of TRPH/TSPH

Fig. 5 examines the outcome of the CAVOA-DLSWC technique in the training and validation process on 80:20 of TRPH/TSPH. The outcome specified that the CAVOA-DLSWC methodology gains better accu_y values with the highest epochs. Moreover, the maximum validation accu_y with training accu_y shows that the CAVOA-DLSWC model effectively learns on 80:20 of TRPH/TSPH.

The loss analysis of the CAVOA-DLSWC technique in training and validation is shown on 80:20 of TRPH/TSPH in Fig. 6. The outcome indicates that the CAVOA-DLSWC model reaches nearby outcomes of training and validation losses. The CAVOA-DLSWC algorithm efficiently learns on 80:20 of TRPH/TSPH.




Figure 5: Accuracy curve of CAVOA-DLSWC model with 80:20 of TRPH/TSPH

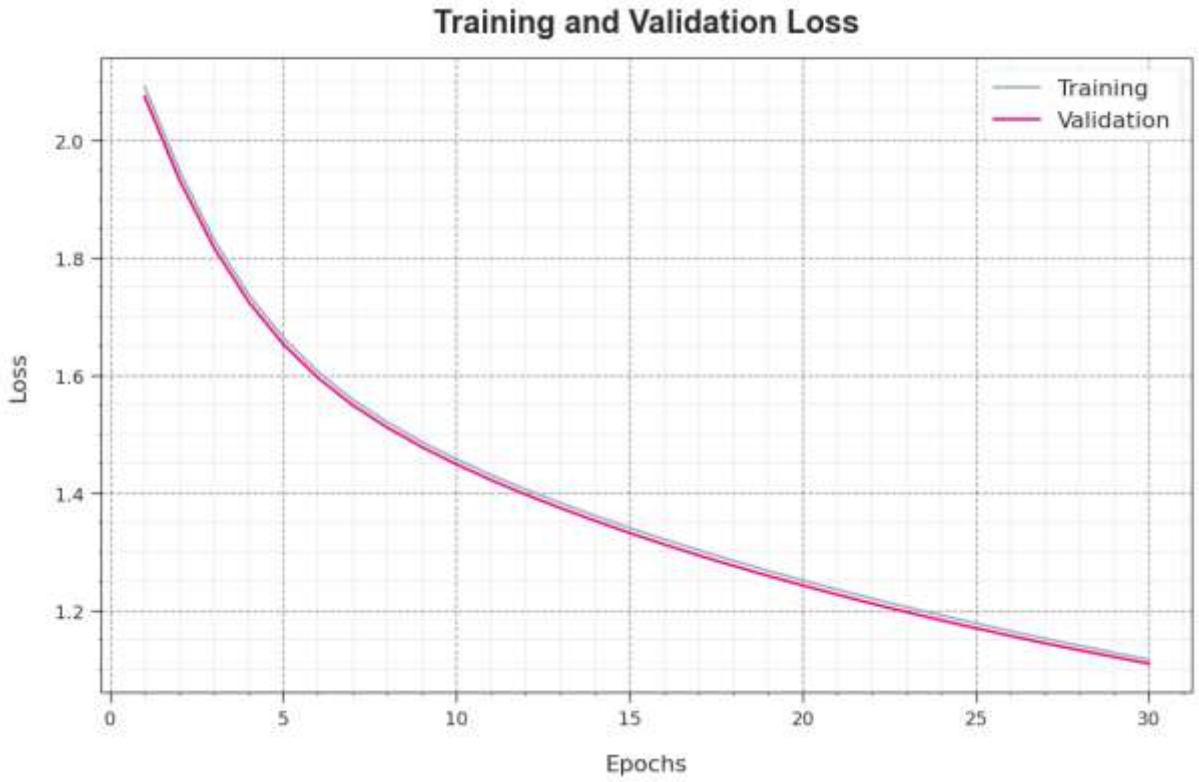



Figure 6: Loss curve of CAVOA-DLSWC model with 80:20 of TRPH/TSPH

A brief PR analysis of the CAVOA-DLSWC system is demonstrated on 80:20 of TRPH/TSPH

in Fig. 7. The outcomes pointed out that the CAVOA-DLSWC algorithm resulted in the highest values of PR. Further, the CAVOA-DLSWC methodology obtains maximum PR outcomes in all classes.

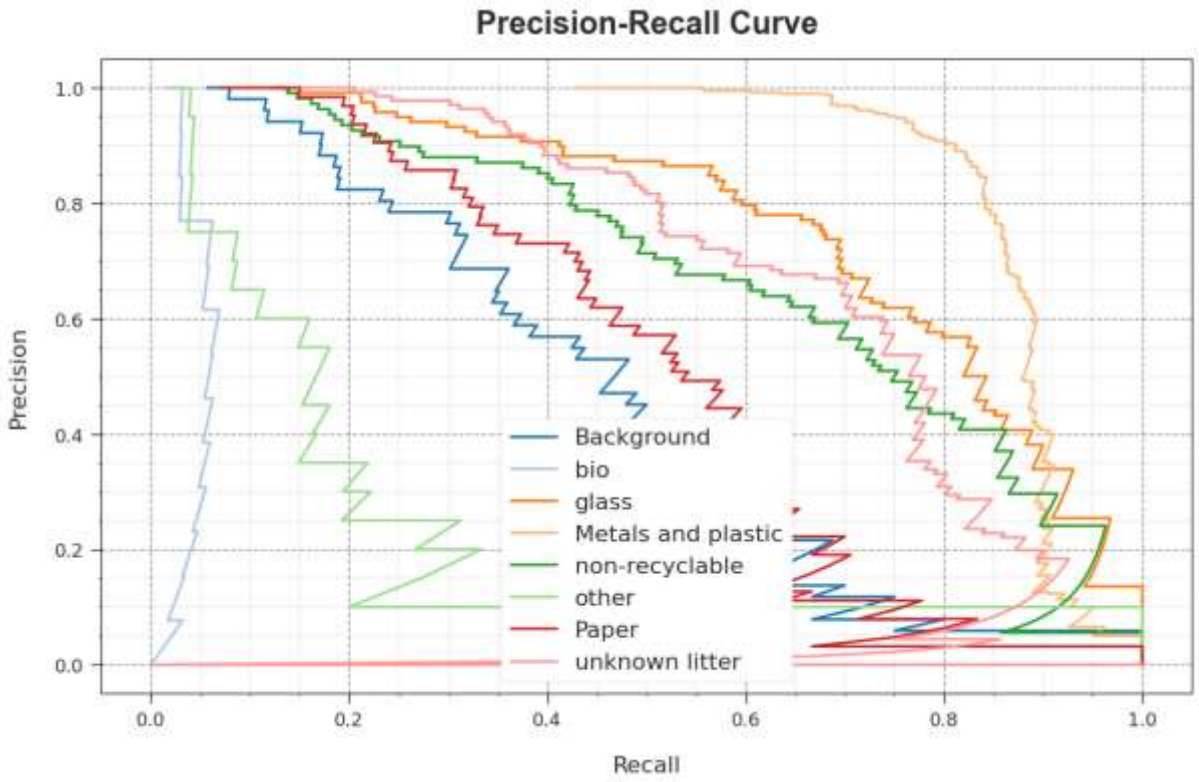



Figure 7: PR curve of CAVOA-DLSWC method on 80:20 of TRPH/TSPH

In Fig. 8, a ROC outcome of the CAVOA-DLSWC approach is demonstrated on 80:20 of TRPH/TSPH. The outcome showed that the CAVOA-DLSWC model resulted in increased ROC values. Furthermore, the CAVOA-DLSWC approach could extend maximum ROC performances on all classes.

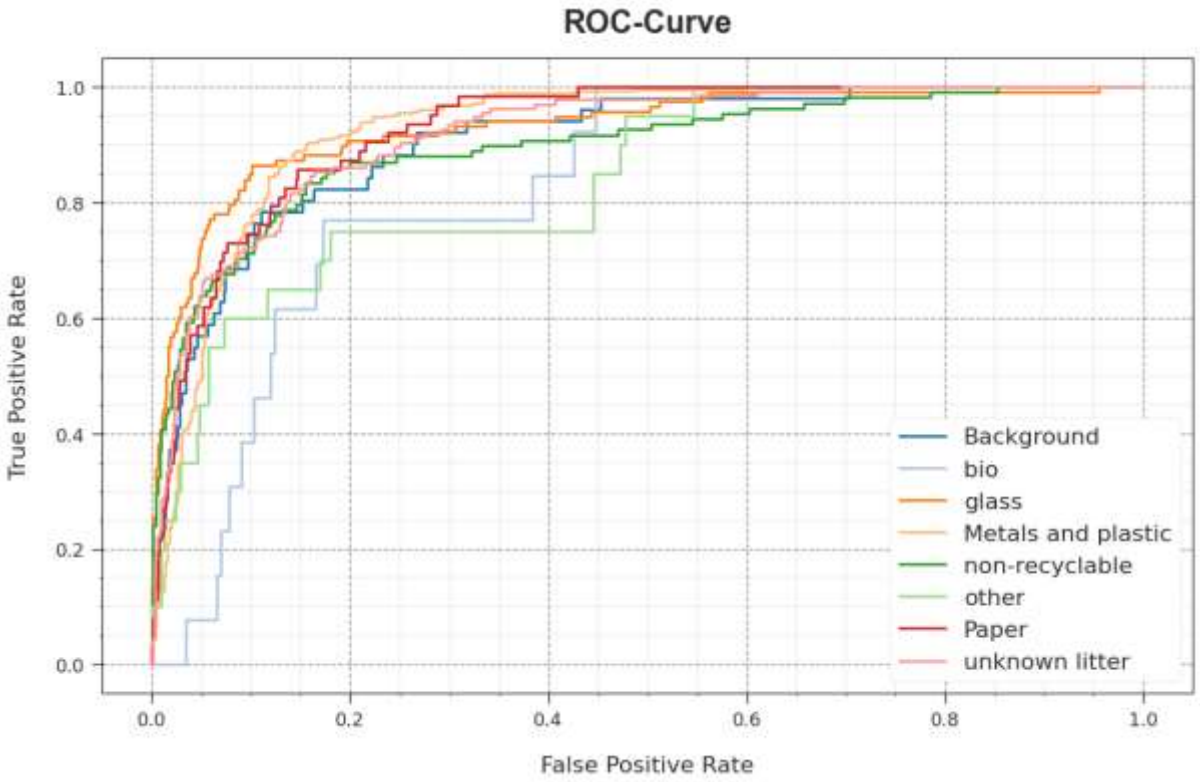



Figure 8: ROC curve of CAVOA-DLSWC approach on 80:20 of TRPH/TSPH

The overall waste classification outcomes of the CAVOA-DLSWC method are described in Table 3 and Fig. 9. The outcome illustrated that the CAVOA-DLSWC algorithm categorized eight types of waste objects accurately. For example, with 70% of TRPH, the CAVOA-DLSWC model obtains average $accu_y$ of 91.30%, $prec_n$ of 47.60%, $spec_y$ of 93.33%, $AUC_{score}$ of 63.31%, and NPV of 95.24%. Also, with 30% of TSPH, the CAVOA-DLSWC system gains average $accu_y$ of 90.84%, $prec_n$ of 45.80%, $spec_y$ of 93.07%, $AUC_{score}$ of 62.70%, and NPV of 94.95%.

**Table 3:** Waste classifier outcome of CAVOA-DLSWC model with 70:30 of TRPH/TSPH

| **Class** | $Accu_y$ | $Prec_n$ | $Spec_y$ | $AUC_{score}$ | **NPV** |
|---|---|---|---|---|---|
| **Training Phase (70%)** | | | | | |
| Background | 93.54 | 80.00 | 99.86 | 53.69 | 93.63 |
| bio | 99.10 | 00.00 | 100.00 | 50.00 | 99.10 |
| glass | 90.04 | 55.20 | 97.99 | 59.68 | 91.50 |
| Metals and plastic | 78.60 | 67.77 | 63.06 | 80.66 | 97.86 |
| non-recyclable | 90.62 | 65.90 | 96.18 | 73.93 | 93.30 |
| other | 96.88 | 00.00 | 100.00 | 50.00 | 96.88 |
| Paper | 93.19 | 52.94 | 99.45 | 53.93 | 93.63 |
| unknown litter | 88.43 | 58.96 | 90.11 | 84.61 | 96.00 |
| **Average** | **91.30** | **47.60** | **93.33** | **63.31** | **95.24** |
| **Testing Phase (30%)** | | | | | |
| Background | 93.33 | 75.00 | 99.84 | 53.15 | 93.44 |
| bio | 99.18 | 00.00 | 100.00 | 50.00 | 99.18 |

| | | | | | |
|---|---|---|---|---|---|
| glass | 90.11 | 57.41 | 98.08 | 60.11 | 91.49 |
| Metals and plastic | 77.38 | 66.12 | 61.87 | 79.81 | 97.30 |
| non-recyclable | 90.56 | 70.23 | 96.63 | 74.01 | 92.77 |
| other | 97.53 | 00.00 | 100.00 | 50.00 | 97.53 |
| Paper | 91.76 | 44.44 | 99.59 | 51.63 | 92.08 |
| unknown litter | 86.89 | 53.21 | 88.53 | 82.87 | 95.83 |
| **Average** | **90.84** | **45.80** | **93.07** | **62.70** | **94.95** |

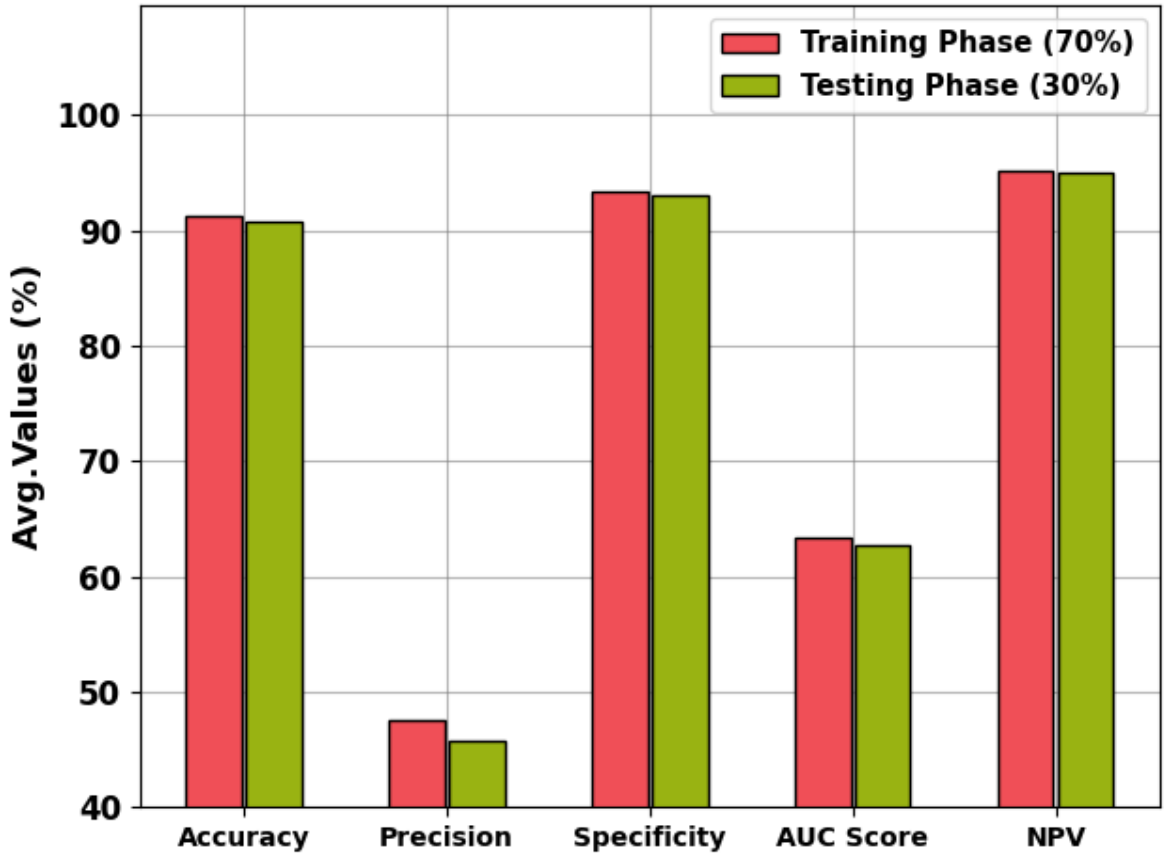



Figure 9: Average outcome of CAVOA-DLSWC model on 70:30 of TRPH/TSPH

Fig. 10 examines the accuracy of the CAVOA-DLSWC approach under training and validation process on 70:30 of TRPH/TSPH. The outcome indicated that the CAVOA-DLSWC technique obtains maximum accu_y values with the highest epochs. Moreover, the maximum validation accu_y with training accu_y reveals that the CAVOA-DLSWC model efficiently learns on 70:30 of TRPH/TSPH.

The loss outcome of the CAVOA-DLSWC model under training and validation is shown on 70:30 of TRPH/TSPH in Fig. 11. The outcome shows that the CAVOA-DLSWC system gains nearby outcomes of training and validation losses. The CAVOA-DLSWC algorithm efficiently learns on 70:30 of TRPH/TSPH.




Figure 10: Accuracy curve of CAVOA-DLSWC methodology on 70:30 of TRPH/TSPH

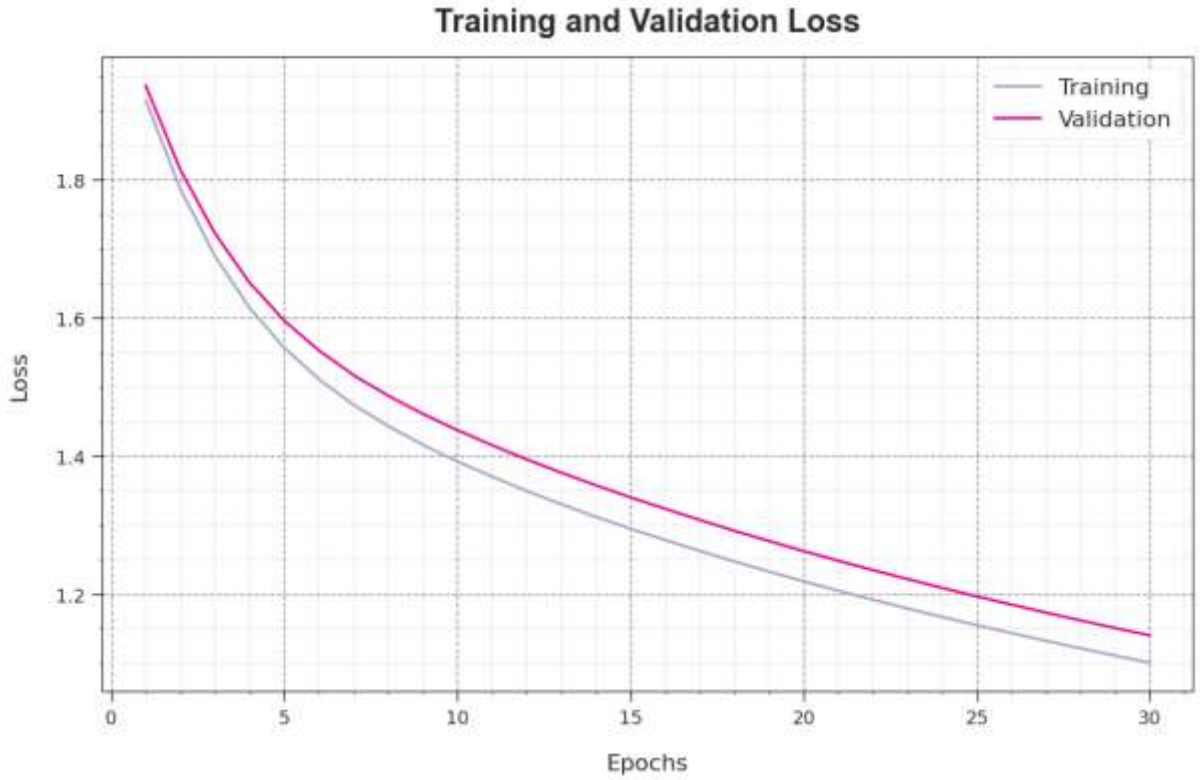



Figure 11: Loss curve of CAVOA-DLSWC approach with 70:30 of TRPH/TSPH

A brief PR analysis of the CAVOA-DLSWC system is exposed on 70:30 of TRPH/TSPH in

Fig. 12. The outcome showed that the CAVOA-DLSWC model resulted in maximum values of PR. Furthermore, the CAVOA-DLSWC method obtains maximum PR values on all classes.

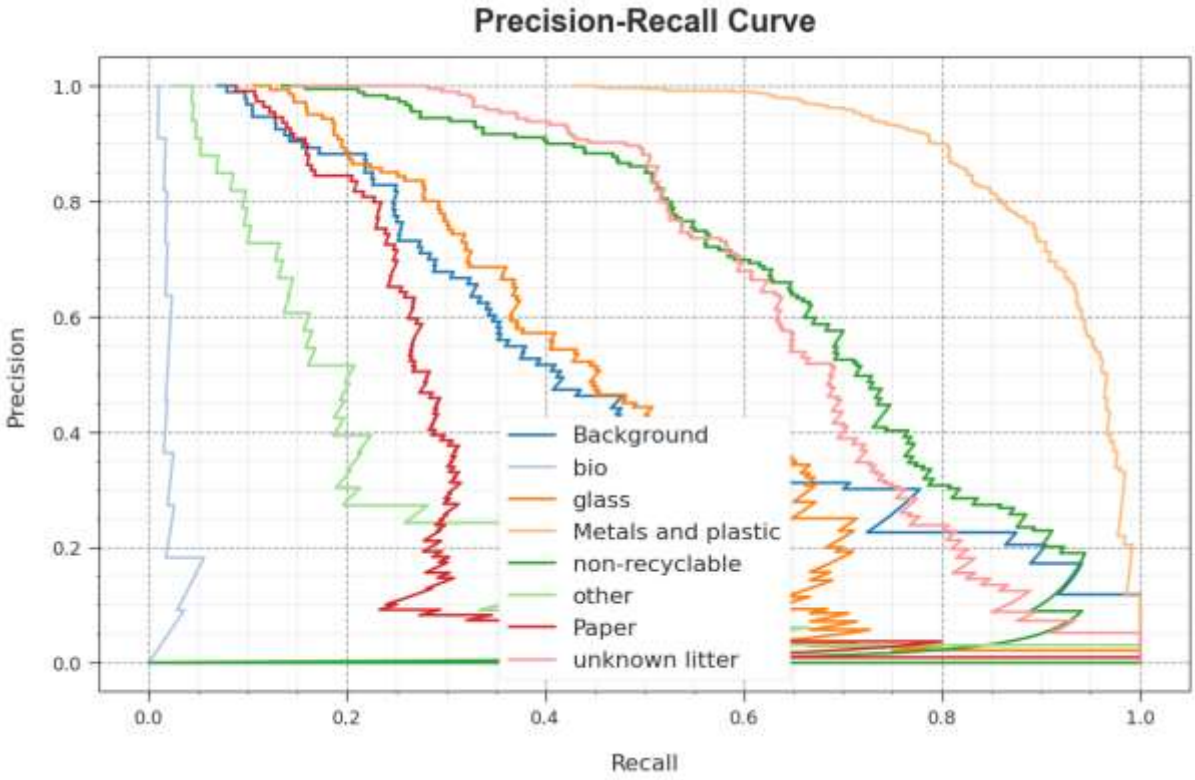



Figure 12: PR curve of CAVOA-DLSWC methodology with 70:30 of TRPH/TSPH

In Fig. 13, a ROC analysis of the CAVOA-DLSWC algorithm is shown at 70:30 of TRPH/TSPH. The outcome showed that the CAVOA-DLSWC model resulted in the highest ROC values. Moreover, the CAVOA-DLSWC approach extends improved ROC values under all classes.

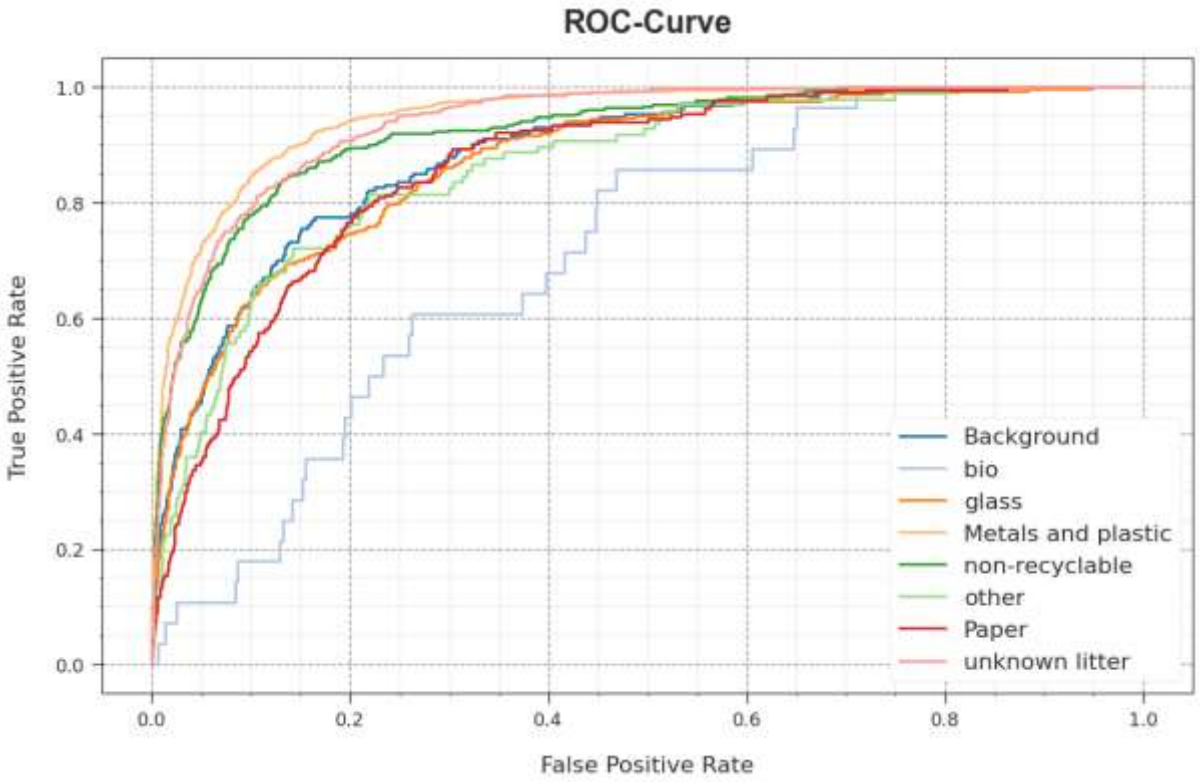



Figure 13: ROC curve of CAVOA-DLSWC approach with 70:30 of TRPH/TSPH

A comparative $accu_y$ assessment of the CAVOA-DLSWC algorithm is reported in Table 4 and Fig. 14 [1]. The figure implied that the CAVOA-DLSWC method reaches a maximum $accu_y$ of 91.30%. On the contrary, the existing DL-PWCS, AlexNet, MobileNetv1 and MobileNetv2 models accomplish reduced $accu_y$ of 74%, 72%, 80%, and 86% correspondingly.

**Table 4**: $Accu_y$ analysis of CAVOA-DLSWC approach with recent algorithms

| **Methods** | **Accuracy (%)** |
|---|---|
| CAVOA-DLSWC | 91.30 |
| DL-PWCS | 74.00 |
| AlexNet | 72.00 |
| MobileNetv1 | 80.00 |
| MobileNetv2 | 86.00 |

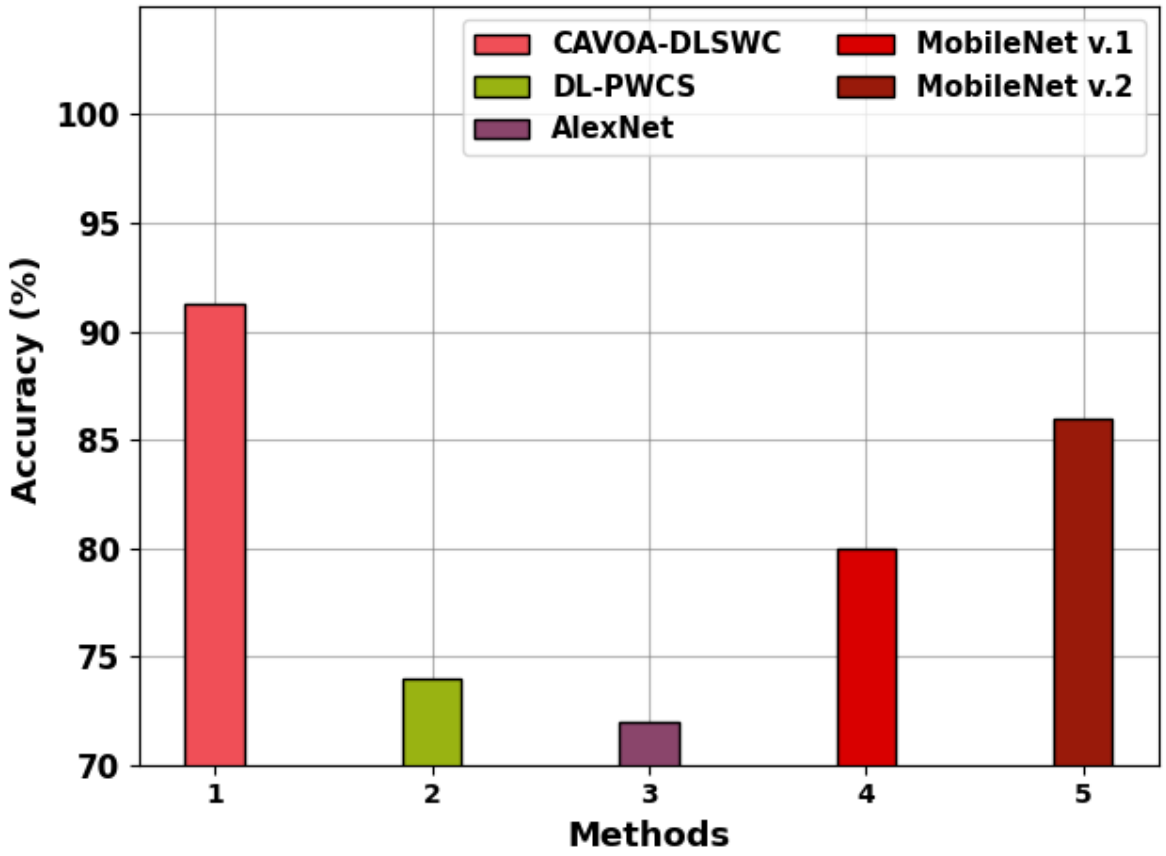



Figure 14: Accuracy analysis of CAVOA-DLSWC approach with recent algorithms

A comparative CT assessment of the CAVOA-DLSWC approach is reported in Table 5 and Fig. 15. The outcomes inferred that the CAVOA-DLSWC method reaches a reduced CT of 10.17s. In contrast, the existing DL-PWCS, AlexNet, MobileNetv1 and MobileNetv2 algorithms accomplish increased CT of 19.20s, 20.10s, 14.9s, and 23s correspondingly.

**Table 5:** CT analysis of CAVOA-DLSWC approach with recent algorithms

| **Methods** | **Computational Time (sec)** |
|---|---|
| CAVOA-DLSWC | 10.17 |
| DL-PWCS | 19.20 |
| AlexNet | 20.10 |
| MobileNet v.1 | 14.90 |
| MobileNet v.2 | 23.00 |

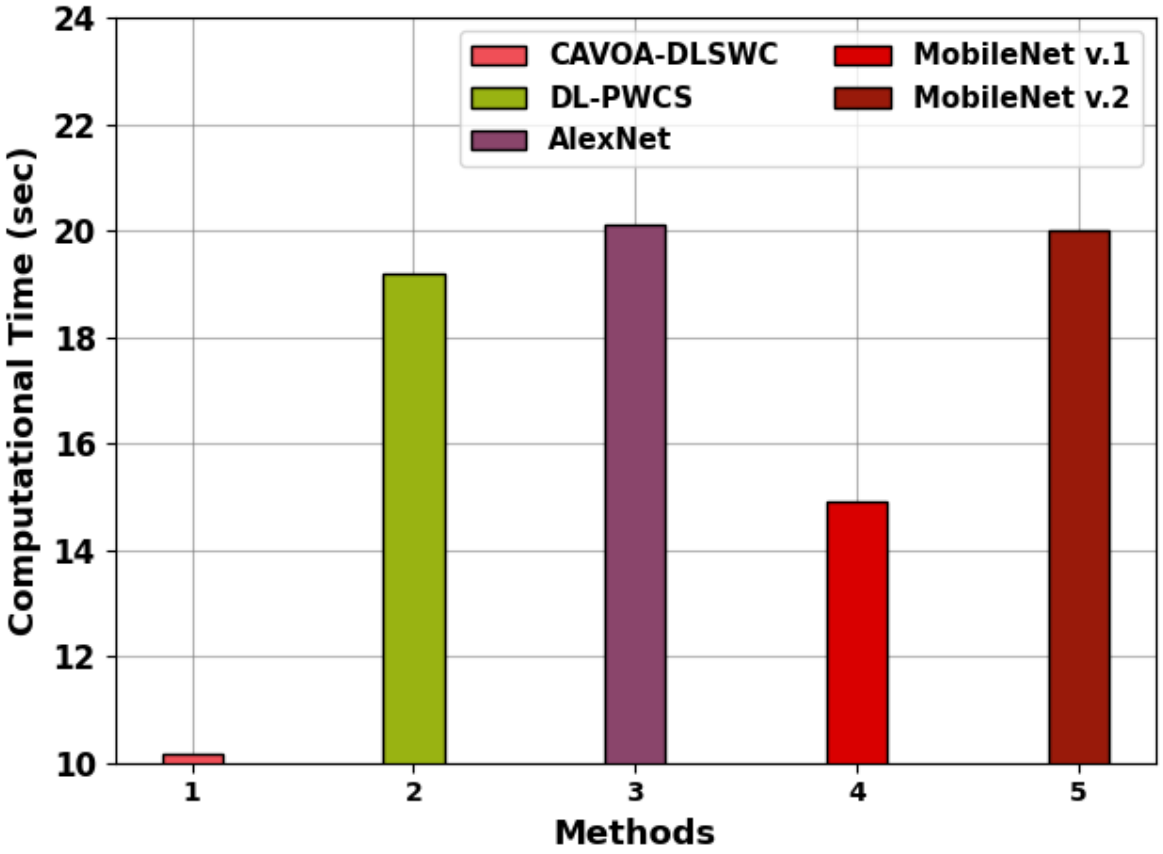



Figure 15: CT analysis of CAVOA-DLSWC method with current methods

These experimental analyses highlighted the enhanced waste classification outcome of the CAVOA-DLSWC algorithm.

## 5. Conclusion

In this study, we have presented a novel CAVOA-DLSWC approach for a robust waste classification algorithm, which helps to improve recycling productivity. The CAVOA-DLSWC method follows a three-stage process: Lightweight RetinaNet object detector, CAVOA-based hyperparameter tuning, and CLSTM-based object classification. The CAVOA is derived by integrating the chaotic concepts into the initial iteration values of the AVOA. Once the waste objects are identified, the classification process can be performed with the use of the CLSTM approach. The experimental values of the CAVOA-DLSWC algorithm can be tested using the solid waste dataset comprising diverse kinds of waste objects. The comparative results show the higher solution of the CAVOA-DLSWC model over other existing techniques. In the future, the proposed CAVOA-DLSWC technique has been tested on large-scale real-time waste datasets.

## References

[1] Zhou, X., Xu, X., Liang, W., Zeng, Z., Shimizu, S., Yang, L.T., & Jin, Q. (2021). Intelligent small object detection for digital twin in smart manufacturing with industrial cyber-physical systems. IEEE Transactions on Industrial Informatics, 18(2), 1377-1386.

[2] Blömeke, S., Rickert, J., Mennenga, M., Thiede, S., Spengler, T.S., & Herrmann, C. (2020). Recycling 4.0–Mapping smart manufacturing solutions to remanufacturing and recycling operations. Procedia CIRP, 90, 600-605.

[3] Shaikh, A., Shinde, S., Rondhe, M., & Chinchanikar, S. (2022). Machine Learning Techniques for Smart

Manufacturing: A Comprehensive Review. Industry 4.0 and Advanced Manufacturing: Proceedings of I-4 AM 2022, 127-137.

[4] Andhy Panca Saputra, K. (2021). Waste Object Detection and Classification using Deep Learning Algorithms: YOLOv4 and YOLOv4-tiny. Turkish Journal of Computer and Mathematics Education (TURCOMAT), 12(14), 1666-1677.

[5] Verma, V., Gupta, D., Gupta, S., Uppal, M., Anand, D., Ortega-Mansilla, A., Alharithi, F.S., Almotiri, J., & Goyal, N. (2022). A deep learning-based intelligent garbage detection system using an unmanned aerial vehicle. Symmetry, 14(5), 960.

[6] Rahman, M.W., Islam, R., Hasan, A., Bithi, N.I., Hasan, M.M., & Rahman, M.M. (2022). Intelligent waste management system using deep learning with IoT. Journal of King Saud University-Computer and Information Sciences, 34(5), 2072-2087.

[7] Nguyen, X.C., Nguyen, T.T.H., La, D.D., Kumar, G., Rene, E.R., Nguyen, D.D., Chang, S.W., Chung, W.J., Nguyen, X.H., & Nguyen, V.K. (2021). Development of machine learning-based models to forecast solid waste generation in residential areas: A case study from Vietnam. Resources, Conservation and Recycling, 167, 105381.

[8] Sannigrahi, S., Basu, B., Basu, A.S., & Pilla, F. (2022). Development of automated marine floating plastic detection system using Sentinel-2 imagery and machine learning models. Marine Pollution Bulletin, 178, 113527.

[9] Yan, B., Liang, R., Li, B., Tao, J., Chen, G., Cheng, Z., Zhu, Z., & Li, X. (2021). Fast identification and characterization of residual wastes via laser-induced breakdown spectroscopy and machine learning. Resources, Conservation and Recycling, 174, 105851.

[10] Zhang, Q., Yang, Q., Zhang, X., Bao, Q., Su, J., & Liu, X. (2021). Waste image classification based on transfer learning and convolutional neural network. Waste Management, 135, 150-157.

[11] Alsubaei, F.S., Al-Wesabi, F.N., & Hilal, A.M. (2022). Deep learning-based small object detection and classification model for garbage waste management in smart cities and iot environment. Applied Sciences, 12(5), 2281.

[12] Wang, C., Qin, J., Qu, C., Ran, X., Liu, C., & Chen, B. (2021). A smart municipal waste management system based on deep-learning and Internet of Things. Waste Management, 135, 20-29.

[13] Malik, M., Sharma, S., Uddin, M., Chen, C.L., Wu, C.M., Soni, P., & Chaudhary, S. (2022). Waste Classification for Sustainable Development Using Image Recognition with Deep Learning Neural Network Models. Sustainability, 14(12), 7222.

[14] Agbehadji, I.E., Abayomi, A., Bui, K.H.N., Millham, R.C., & Freeman, E. (2022). Nature-Inspired Search Method and Custom Waste Object Detection and Classification Model for Smart Waste Bin. Sensors, 22(16), 6176.

[15] Khan, R., Kumar, S., Srivastava, A.K., Dhingra, N., Gupta, M., Bhati, N., & Kumari, P. (2021). Machine learning and IoT-based waste management model. Computational Intelligence and Neuroscience, 2021.

[16] Abu-Qdais, H., Shatnawi, N., & Esra'a, A.A. (2023). Intelligent solid waste classification system using a combination of image processing and machine learning models.

[17] Cheng, Y., Ekici, E., Yildiz, G., Yang, Y., Coward, B., & Wang, J. (2023). Applied machine learning for the prediction of waste plastic pyrolysis towards valuable fuel and chemicals production. Journal of Analytical and Applied Pyrolysis, 105857.

[18] Li, Y., Dua, A., & Ren, F. (2020). Lightweight retinanet for object detection on edge devices. In IEEE 6th World Forum on Internet of Things (WF-IoT), New Orleans, LA, USA, pp. 1–6.

[19] Al-Dhaifallah, M. (2023). Analytical solutions using special trans functions theory for current–voltage expressions of perovskite solar cells and their approximate equivalent circuits. Ain Shams Engineering Journal, 102225.

[20] Zheng, H., Lin, F., Feng, X., & Chen, Y. (2020). A hybrid deep learning model with attention-based conv-LSTM networks for short-term input data prediction. IEEE.